Dalton Transactions

ROYAL SOCIETY OF CHEMISTRY

PAPER

View Article Online
View Journal | View Issue

Cite this: *Dalton Trans.*, 2023, **52**, 15757

In vivo and *in vitro* studies of $[M(\eta^6\text{-pseudoerlotinib})_2]^+$ sandwich complexes (M = Re, ^{99m}Tc)†

Federica Battistin, *[a] Célia Fernandes,[b] Paula. D. Raposinho,[b] Olivier Blacque,[a] António Paulo*[b] and Roger Alberto[a]

Received 14th September 2023,
Accepted 11th October 2023

DOI: 10.1039/d3dt03011c

rsc.li/dalton

The pursuit of molecular imaging for tumors has led to endeavors focused on targeting epidermal growth factor receptors (EGFR) through monoclonal antibodies or radionuclide-labelled EGF analogs with ^{99m}Tc, ^{111}In, or ^{131}I. In this context, various ^{99m}Tc-labeled EGFR inhibitors using quinazoline structures have been reported based on the so-called pendant approach and on two types of complexes and labelling strategies: "4 + 1" mixed ligand complexes and *fac*-tricarbonyl complexes. Apart from this approach, which alters lead structures by linking pharmacophores to chelator frameworks through different connectors, the integrated incorporation of topoisomerase and tyrosine kinase inhibitors into Re and ^{99m}Tc complexes has not been explored. Here we present $[M(\eta^6\text{-inhibitor})_2]^+$ (M = Re, ^{99m}Tc) and $[Re(\eta^6\text{-bz})(\eta^6\text{-inhibitor})]^+$ complexes, where the core structure of an EGFR tyrosine kinase inhibitor binds directly to the metal center. These complexes exhibit potential for tumor imaging: initial biological investigations highlight the influence of one *versus* two bound inhibitors on the metal center.

Introduction

DNA topoisomerases are nuclear enzymes that catalyze the introduction of topological changes to the DNA strand. They are essential for proliferating cells since they release the tension of DNA during replication and transcription by formation of transient single-stranded (*i.e.* type I topoisomerases) or double-stranded (*i.e.* type II topoisomerases) breaks in the DNA double helix.[1,2] An effective target in the treatment of a large number of cancers is human topoisomerase II (topo II).[3,4] The epidermal growth factor receptor (EGFR) is another relevant target for cancer therapy, being overexpressed in many cancers such as ovary, breast and lung cancer and having a regulatory role in their growth.[5–7] Moreover, high levels of EGFR have been shown to be linked to the development of resistance of cancer cells to topo II inhibitors.[8] Therefore, a simultaneous inhibition of topo II and EGFR might be an effective strategy for anticancer treatment. Several classes of EGFR tyrosine kinase inhibitors have been reported and,[9] among them, the most potent, selective and approved for clinical use are Iressa®/Gefitinib and Tarceva®/Erlotinib (Fig. 1) which are quinazoline-type EGFR inhibitors and also act on topoisomerases.[8]

Efforts have been made to achieve molecular imaging of tumor based on the targeting of EGFR receptors with monoclonal antibodies or EGF analogues labeled with radionuclides such as ^{99m}Tc, ^{111}In, or ^{131}I.[10] For this purpose, radioprobes that utilize tyrosine kinase inhibitors (TKI) as targeting vectors are an attractive alternative, namely to identify patients who would benefit from TKI therapy and for monitoring their response to personalized cancer treatment.[10–16]

Several ^{99m}Tc labelled quinazoline type EGFR inhibitors have been reported in the literature, based on the so-called pendant approach and on two types of complexes and labelling strategies: "4 + 1" mixed ligand complexes and *fac*-tricarbonyl complexes (Fig. 2).[17–20] Many of these ^{99m}Tc complexes

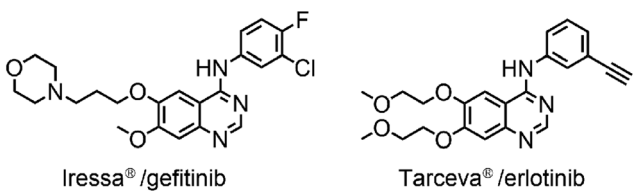

Fig. 1 Two examples of FDA approved quinazoline-type drugs, acting as EGFR and topoisomerase inhibitors.

[a]*Department of Chemistry, University of Zurich, Winterthurerstr. 190, 8057 Zurich, Switzerland. E-mail: federica.battistin@chem.uzh.ch*
[b]*Centro de Ciências e Tecnologias Nucleares, Instituto Superior Técnico, Universidade de Lisboa, Campus Tecnológico e Nuclear, Bobadela, Portugal. E-mail: apaulo@ctn.tecnico.ulisboa.pt*

†Electronic supplementary information (ESI) available: NMR and HR-ESI-MS spectral data, γ-traces and crystallographic details of new compounds. CCDC 2293185–2293187. For ESI and crystallographic data in CIF or other electronic format see DOI: https://doi.org/10.1039/d3dt03011c

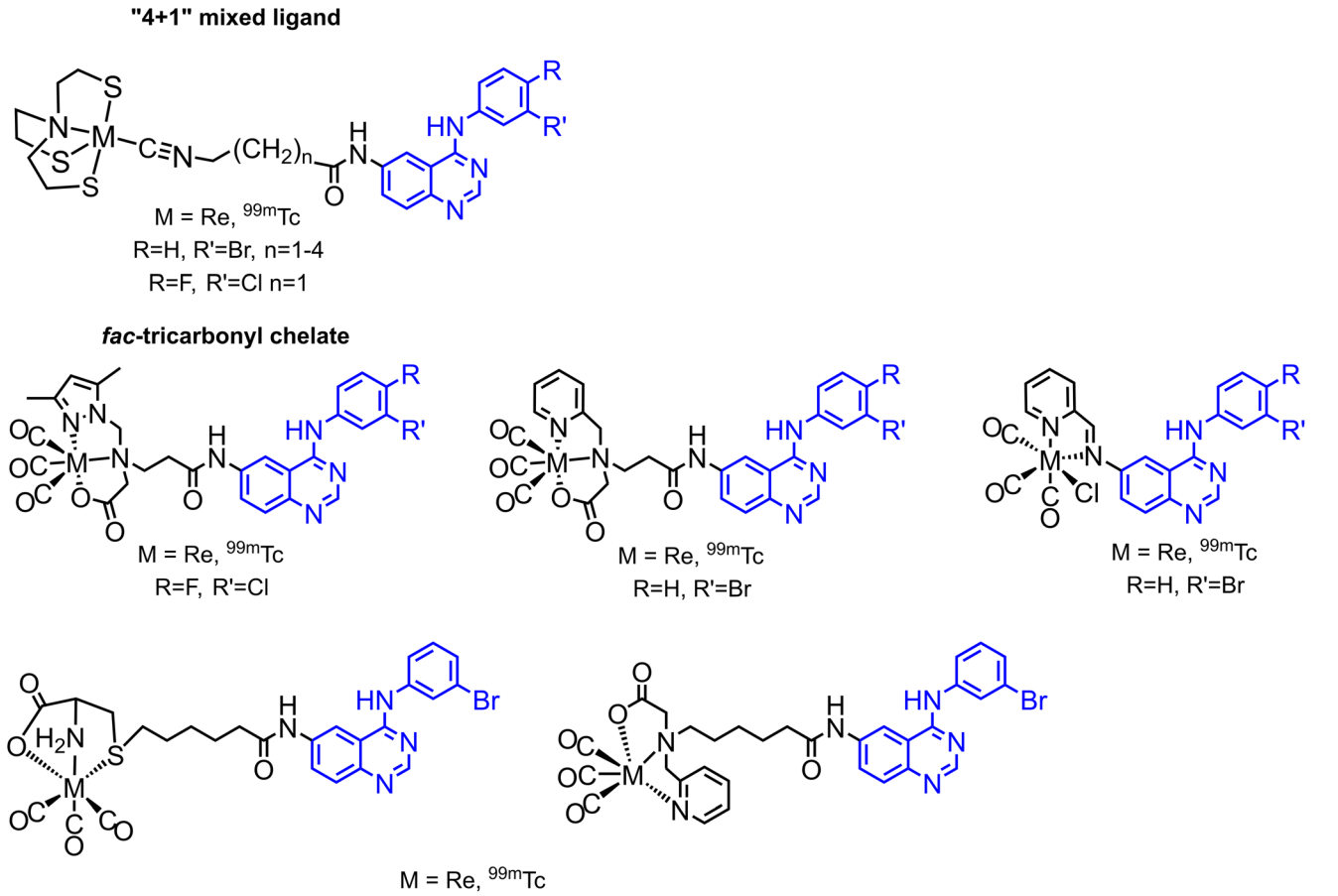

Fig. 2 Literature known ^{99m}Tc labelled quinazoline type EGFR inhibitors.[17–20]

and their Re congeners showed promising results and essentially retained the inhibitory activity of the respective free inhibitors, *i.e.* the parent pharmaceuticals.

Besides the above-mentioned complexes obtained through the pendant approach, which involves the attachment of the pharmacophores to the chelator framework through different linkers leading to altered lead structures, there are no examples of an integrated incorporation of topoisomerases – and tyrosine kinase inhibitors in the structures of Re and ^{99m}Tc complexes. We have recently reported on the direct incorporation of arene-based pharmaceuticals into rhenium complexes by exchanging naphthalene (napht) in $[Re(\eta^6\text{-napht})_2]^+$ and $[Re(\eta^6\text{-bz})(\eta^6\text{-napht})]^+$ (bz = benzene) with highly functionalized arenes, which allows to explore the so-called integrated approach. Naphthalene is weaker bound to rhenium as compared to benzene because of its more extended π-system.[21] This allows its exchange with different functionalized arenes and arene-based pharmaceuticals. The substitution can take place either in pure arenes using a large excess of the arene, or in dioxane with *N*-methyl-pyrrolidone (NMP) as a catalyst and fewer equivalents of the arenes, as shown in Scheme 1.[22,23]

In water, functionalized arenes can be labeled directly to form $[^{99m}Tc(\eta^6\text{-arene})_2]^+$ complexes in a single step starting from $[^{99m}TcO_4]^-$.[22,23] This is possible due to the high dilution of ^{99m}Tc. However, the same procedure cannot be replicated for the rhenium homologues. In both Re and ^{99m}Tc sandwich complexes, the functional groups and one face of the pharmaceutical are left unchanged.

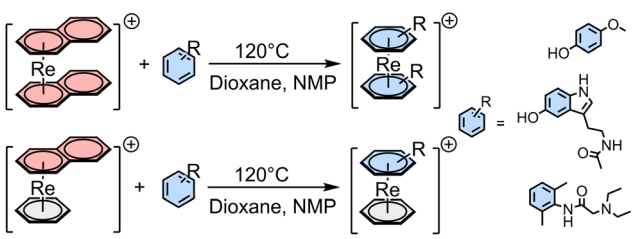

Scheme 1 General pathway for the synthesis of $[Re(\eta^6\text{-arene})_2]^+$ and $[Re(\eta^6\text{-bz})(\eta^6\text{-arene})]^+$ with arene = mequinol, melatonin, lidocaine and others.[22,23]

Following a similar approach, we present herein the preparation of $[M(\eta^6\text{-inhibitor})_2]^+$ (M = Re, ^{99m}Tc) and $[Re(\eta^6\text{-bz})(\eta^6\text{-inhibitor})]^+$ in which the parent structure of an EGFR tyrosine kinase inhibitor is directly coordinated to the metal. We selected quinazoline-type EGFR inhibitors, structurally similar to the approved drug erlotinib. We also report the first biological studies of these sandwich complexes to assess the influ-

ence of having one or two inhibitors bound to a metal center in comparison with the free drug.

Results and discussion

Rhenium complexes

The syntheses of various $[Re(\eta^6\text{-pharm})_2]^+$ complexes with arene-based pharmaceuticals (pharm) have been previously reported by us. Synthetically, naphthalene in $[Re(\eta^6\text{-napht})_2]^+$ was exchanged with the respective pharmaceutical as ligands, comprising an available phenyl group, in the presence of *N*-methyl-pyrrolidone (NMP).[23] Erlotinib has two rings that could eventually replace naphthalene, a quinazoline moiety and an ethynyl aniline (Fig. 1). To selectively synthesize the complex with the rhenium sandwiched by the aniline rings, we started from $[Re(\eta^6\text{-aniline})_2]^+$.[22,24] Conjugation of the fragment **L1** (see Scheme 2) would give a 'pseudoerlotinib' rhenium sandwich through a two steps reaction: (i) synthesis of $[Re(\eta^6\text{-aniline})_2]^+$; (ii) nucleophilic aromatic substitution to form $[Re(\eta^6\text{-pseudoerlotinib})_2]^+$, thereby modifying a procedure reported in literature for the synthesis of the free erlotinib.[25]

$[Re(\eta^6\text{-aniline})_2]^+$ was prepared by exchange of naphthalene with aniline in $[Re(\eta^6\text{-napht})_2]^+$.[24] $[Re(\eta^6\text{-aniline})_2]^+$ was then reacted with **L1** in 0.5 M HCl solution at 70 °C for 24 h, forming $[Re(\eta^6\text{-pseudoerlotinib})_2]^+$ (**1**) in 77% yield (Scheme 2). The ^{1}H NMR spectrum of **1** in acetone-d_6 displays three resonances for the aniline ring at 7.30 (H_o), 6.19 (H_m) and 5.87 (H_p) ppm respectively, which are upfield shifted as compared to the signals of the $[Re(\eta^6\text{-aniline})_2]^+$. The strongest shifted signals are the protons *ortho* to the NH functional group (Δ = 1.42 ppm), followed by *meta* (Δ = 0.49 ppm) and *para* (Δ = 0.36 ppm). The aromatic region of the spectrum shows also three singlets of the quinazoline protons at 8.46, 6.97 and 6.77 ppm respectively. Between 4.5 and 3.7 ppm there are four multiplets of the methylene bridges of **L1** and, finally, two close singlets (3.48 and 3.45 ppm respectively) of the two methoxy functional groups (ESI).

Single crystal X-ray diffraction analysis confirmed the structure of the complex (Fig. 3). Since the crystals spontaneously formed in the reaction mixture (acidic conditions), both ligands are protonated at one of the nitrogen atoms from the quinazoline moiety as clearly visible in the crystal structure, and the overall charge of the complex is 3+.

To compare the biological behavior of Re(I) complexes containing one or two erlotinib analogues, we prepared the mixed

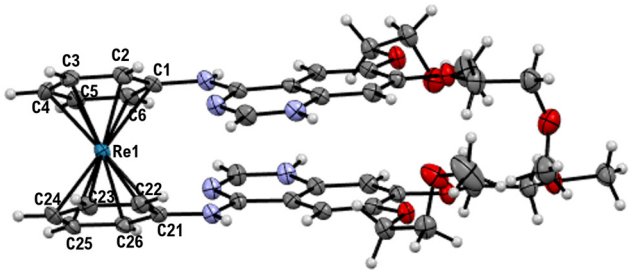

Fig. 3 Ellipsoid displacement plots of protonated $[Re(\eta^6\text{-pseudoerlotinib})_2]^{3+}$ (**1**). Ellipsoids are drawn at 50% probability. $[PF_6]^-$ and $2[Cl]^-$ anions are omitted for clarity. Coordination distances in Ångström (Å): Re1–C1 = 2.259(3), Re1–C2 = 2.250(3), Re1–C3 = 2.241(3), Re1C4 = 2.238(3), Re1C5 = 2.244(3), Re1–C6 = 2.242(3), Re1–C21 = 2.264(3), Re1–C22 = 2.244(3), Re1–C23 = 2.247(3), Re1C24 = 2.244(3), Re1C25 = 2.239(3), Re1–C26 = 2.244(3).

complex $[Re(\eta^6\text{-bz})(\eta^6\text{-pseudoerlotinib})]^+$ adopting the same approach. The reaction between $[Re(\eta^6\text{-bz})(\eta^6\text{-naph})]^+$ and aniline led to $[Re(\eta^6\text{-bz})(\eta^6\text{-aniline})]^+$ (**2**) in 76% yield (Scheme 3). In the ^{1}H NMR spectrum in acetone-d_6 there is a singlet at 5.76 ppm for the six aromatic protons of benzene and three more multiplets at 6.25(H_o), 6.08 (H_m), 5.82 (H_p) ppm respectively for the protons of aniline. The structure was confirmed by single crystals X-ray diffraction analysis (Fig. 4).

As for the synthesis of **1**, a nucleophilic aromatic substitution between **2** and **L1** led to $[Re(\eta^6\text{-bz})(\eta^6\text{-pseudoerlotinib})]^+$ (**3**) in 75% yield (Scheme 3). The ^{1}H NMR spectrum of **2** in acetone-d_6 is very similar to **1**: also in this case the signals of the aniline and benzene are upfield shifted compared to **2**, with a smaller delta: 0.94 for H_o, 0.24 for H_m, 0.23 for H_p which is overlapping with the singlet of the benzene protons (Δ = 0.04 ppm).

X-ray diffraction performed on single crystals of **3** allowed us to confirm the geometry of the complex (Fig. 4).

Finally, we also prepared the 'pseudoerlotinib' (**L2**) analogue, corresponding to the arene ligands coordinated to rhenium in complex **1** and **3**, to compare the activities of the free molecule with the ones being coordinated to the rhenium complexes, following a literature procedure.[25]

^{99m}Tc sandwich complexes

We reported earlier the direct labelling of arene-containing pharmaceuticals with ^{99m}Tc in water.[23] Since erlotinib has two different arene rings principally accessible for η^6-coordination,

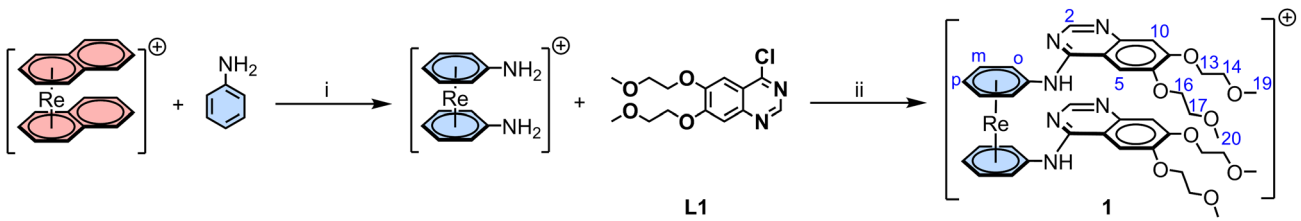

Scheme 2 Two steps synthesis of $[Re(\eta^6\text{-pseudoerlotinib})_2]^+$ (**1**): (i) 120 °C, dioxane, 5 eq. NMP; (ii) 0.5 M HCl, 70 °C.

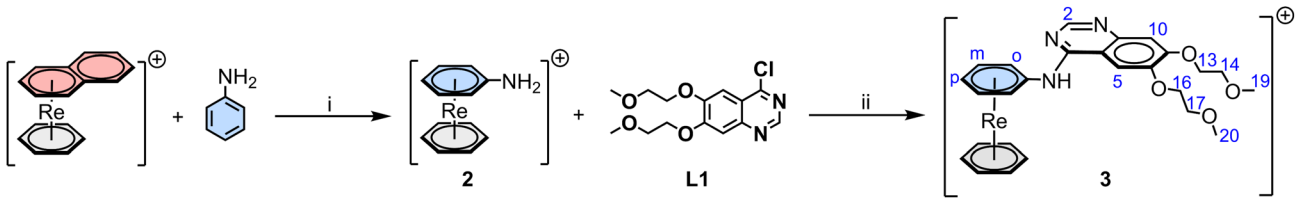

Scheme 3 Two steps synthesis of $[Re(\eta^6\text{-bz})(\eta^6\text{-pseudoerlotinib})]^+$ (**1**): (i) 120 °C, dioxane, 2.5 eq. NMP (**2**); (ii) 0.5 M HCl, 70 °C.

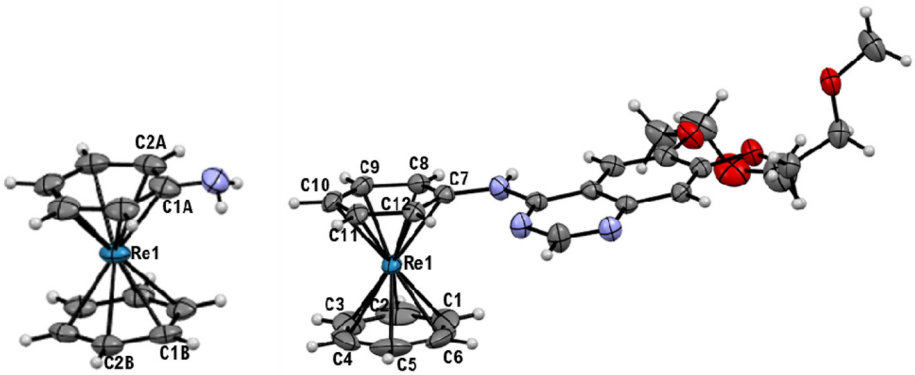

Fig. 4 Ellipsoid displacement plots of $[Re(\eta^6\text{-bz})(\eta^6\text{-aniline})]^+$ (**2**, left) and $[Re(\eta^6\text{-bz})(\eta^6\text{-pseudoerlotinib})]^+$ (**3**, right). Ellipsoids are drawn at 50% probability. $[PF_6]^-$ anions are omitted for clarity. Coordination distances in Ångström (Å) for **2**: Re1–C1A = 2.249(4), Re1–C2A = 2.235(4), Re1–C1B = 2.240(3), Re1C2B = 2.200(3). Coordination distances in Ångström (Å) for **3**: Re1–C1 = 2.214(4), Re1–C2 = 2.206(4), Re1–C3 = 2.222(4), Re1–C4 = 2.222(4), Re1–C5 = 2.226(4), Re1–C6 = 2.227(4), Re1–C7 = 2.305(3), Re1–C8 = 2.239(3), Re1–C9 = 2.235(4), Re1–C10 = 2.241(3), Re1–C11 = 2.229 (3), Re1–C12 = 2.248(3).

a one pot labeling could potentially yield a mixture of labeled compounds: (i) ^{99m}Tc between both aniline rings; (ii) ^{99m}Tc between both quinazoline rings; (iii) mixed compound in which ^{99m}Tc is between aniline and quinazoline rings (Fig. 5). To avoid the formation of this mixture, which would be difficult to separate in radio-HPLC, we followed the two steps

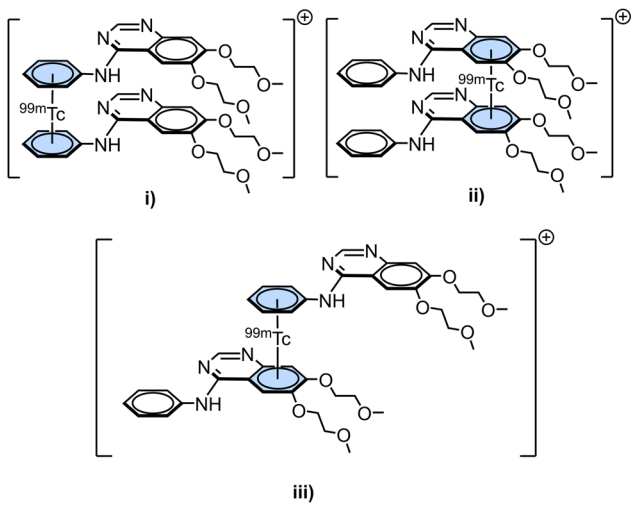

Fig. 5 All possible $[^{99m}Tc(\eta^6\text{-pseudoerlotinib})_2]^+$ complexes that could form with one pot labeling of pseudoerlotinib.

synthesis as in the case of Re for the preparation of $[^{99m}Tc(\eta^6\text{-pseudoerlotinib})_2]^+$.

As for the rhenium complexes, we first labeled aniline by mixing $[^{99m}Tc][TcO_4]^-$ as eluted from a ^{99}Mo/^{99m}Tc generator with aniline in water, using Zn° as reducing agent under acidic conditions to yield $[^{99m}Tc(\eta^6\text{-aniline})_2]^+$in 63% radiochemical yield (RCY), following a procedure already reported by us.[22] After HPLC purification, nucleophilic aromatic substitution between $[^{99m}Tc(\eta^6\text{-aniline})_2]^+$ and **L1** led to $[^{99m}Tc(\eta^6\text{-pseudoerlotinib})_2]^+$ (**[^{99m}Tc]1**) in 62% RCY over two steps of reaction (Scheme 4).

Corroboration of the structure of the ^{99m}Tc complex was performed by comparative HPLC analysis with the homologous Re complex **1**. Fig. 6 shows the co-injection run of **1** and **[^{99m}Tc]1**.

Following the same approach, we attempted to prepare the mixed complex $[^{99m}Tc(\eta^6\text{-bz})(\eta^6\text{-aniline})]^+$, precursor for the synthesis of $[^{99m}Tc(\eta^6\text{-bz})(\eta^6\text{-pseudoerlotinib})]^+$, by reaction of $[^{99m}Tc][TcO_4]^-$ with aniline and benzene in water. Due to the insolubility of benzene in water, the mixed complex was not obtained but only the $[^{99m}Tc][Tc(\eta^6\text{-aniline})_2]^+$ complex.

Finally, we have studied the *in vitro* stability of **[^{99m}Tc]1** in phosphate-buffered saline (PBS) and cell culture medium at 37 °C for 24 h. The radiocomplex remained stable under the tested conditions, as shown by HPLC analysis of the resulting solutions (Fig. S13, ESI†), which prompted its use in the intended biological studies described below.

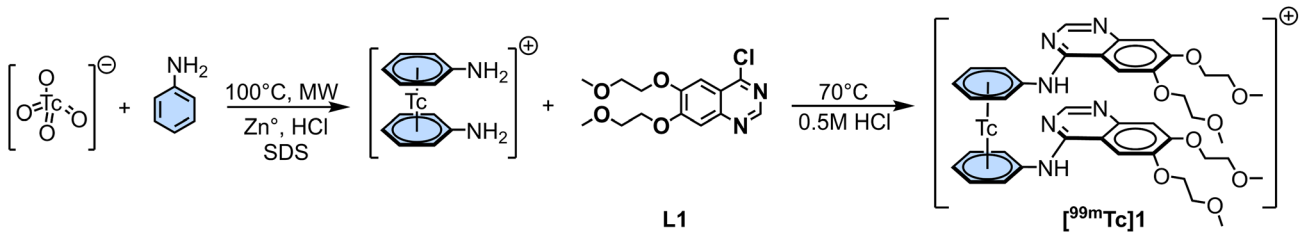

Scheme 4 Two steps synthesis of $[^{99m}Tc(\eta^6\text{-pseudoerlotinib})_2]^+$ (**[^{99m}Tc]1**): (i) synthesis of $[^{99m}Tc(\eta^6\text{-aniline})_2]^+$; (ii) nucleophilic aromatic substitution between $[^{99m}Tc(\eta^6\text{-aniline})_2]^+$ and **L1** to form **[^{99m}Tc]1**.[26]

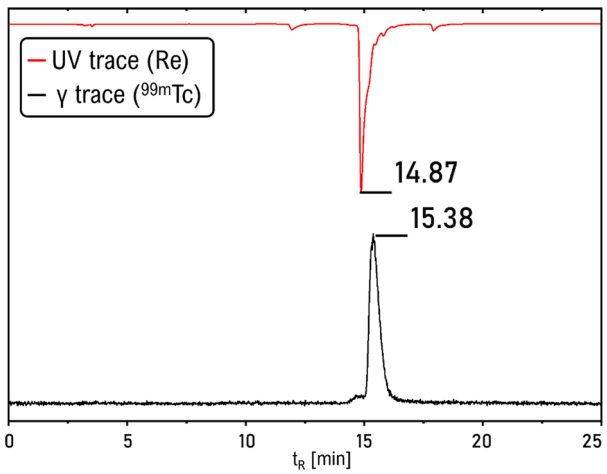

Fig. 6 Co-injection of **1** (top) together with the homologue **[^{99m}Tc]1** (bottom).

Biological studies

Inhibition of tumor cell proliferation. The rhenium complexes **1** and **3** and the ligand **L2** were evaluated for their potency to inhibit the growth of A431 cells (epidermoid carcinoma) by the [1-(4,5-dimethylthiazol-2-yl)-2,5-diphenyl tetrazolium] (MTT) colorimetric assay. As shown in Table 1, the free ligand **L2** has the lowest IC_{50} value (23 μM); complex **1** also presents a value in the μM range (55.72 μM) that is around twice the IC_{50} value of **L2**, showing that the "symmetric" association of two **L2** ligands to the metal did not strongly affect the cytotoxicity of this "pseudoerlotinib" compounds. By contrast, the mixed compound **3** showed a very low capacity of inhibiting cell growth (IC_{50} > 600 μM).

Compared with erlotinib and the reported Re quinazoline type EGFR inhibitors,[17–20] **1** and **L2** showed lower cell growth inhibition towards A431 cell lines. Despite the moderate cytotoxic activity found for **1**, the first Re sandwich complex that directly incorporates an EGFR and a tyrosine kinase inhibitor, it serves as a proof of concept for this type of approach.

Cellular uptake studies. The uptake and accumulation of the metal in cells plays a significant role in determining the cytotoxic activity of metallodrugs. To rationalize the results of the cytotoxicity studies, cellular uptake experiments of $[Re(\eta^6\text{-pseudoerlotinib})_2]^+$ and $[Re(\eta^6\text{-bz})(\eta^6\text{-pseudoerlotinib})]^+$ were performed in the A431 cell lines.

After incubation of the cells with the complexes for 24 h, cell extracts were collected and the intracellular accumulation of Re was measured with inductively coupled plasma mass spectrometry (ICP-MS). The normalized results of the cellular uptake studies are presented in Fig. 7. Complex **1** shows an accumulation which is double compared with compound **3**.

Table 1 IC_{50} values for the inhibition of A431 cell growth by rhenium complexes and the metal free analogues

Compound	IC_{50} [a] (μM)
1	55.72 ± 14.11
3	688.7 ± 6.01
L2	23.23 ± 4.16
Erlotinib	8.31 ± 1.96

[a] Dose–response curves were determined at 0.01, 0.05, 0.1, 0.5, 1, 5, 10, 20, 50, 100 concentrations. The IC_{50} values are the concentration (μM) needed to inhibit cell growth by 50%. IC_{50} values for each derivative were obtained from six independent experiments and are represented as mean ± standard deviation.

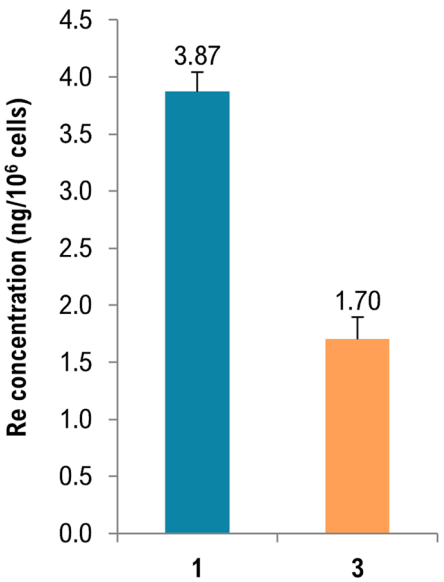

Fig. 7 Cell accumulation of rhenium in A431 cells after exposure to $[Re(\eta^6\text{-pseudoerlotinib})_2]^+$ and $[Re(\eta^6\text{-bz})(\eta^6\text{-pseudoerlotinib})]^+$ (50 μM, 24 h of incubation). The rhenium content is normalized to the cell number and it is represented as mean ± SD (n = 3).

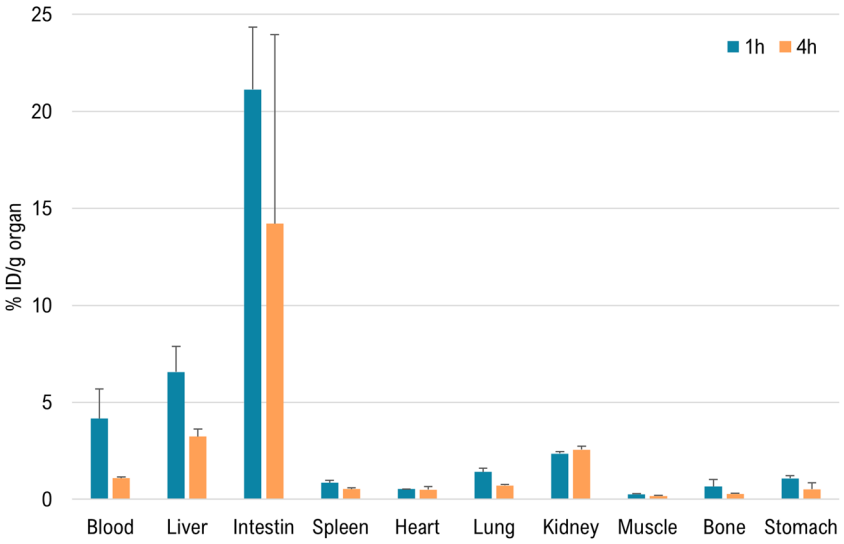

Fig. 8 Biodistribution data expressed as % ID per g organ for [^{99m}Tc]**1** at 1 and 4 h after administration in CD-1 mice (n = 3).

This result is in line with the cytotoxicity studies and with the lower IC_{50} values of **1** compared to **3**. The reasons for the different cellular uptake of complexes **1** and **3** are not clear. It eventually reflects the presence of a larger number of polar ether groups that favor the interaction with outer parts of the cell membrane, followed by diffusion through the cell membrane as specific mechanisms of uptake are not expected for this class of complexes.

Biodistribution and stability studies. Biodistribution study of [^{99m}Tc]**1** was carried out in healthy CD-1 mice at 1 and 4 h post-injection to get a first insight on the biokinetics profile of the ^{99m}Tc labelled compound. Results of these studies are summarized in Fig. 8. The main features of the *in vivo* behavior are the relatively fast clearance from the blood (4.2 ± 1.5 and 1.1 ± 0.1% ID per g for 1 h and 4 h, respectively) and high liver uptake (6.6 ± 1.3 and 3.2 ± 0.4% for 1 h and 4 h, respectively) that clears into the intestines (21.1 ± 3.2 and 14.0 ± 6.9% for 1 h and 4 h, respectively). The percentage of total excretion was 13.4 ± 3.5 and 32.9 ± 17.8 for 1 h and 4 h, respectively. These findings suggest that excretion occurs mainly *via* the hepatobiliary tract, a pattern of excretion most likely due to the high lipophilicity of the compound ($\log D$ = 2.48). Nevertheless, there is a small contribution of excretion through the urinary tract (2.4 ± 0.1% ID per g kidney, at 1 h post injection, which increases to 2.6 ± 0.2% ID per g kidney at 4 h). At 4 h post injection, there is no noteworthy radioactivity retention in any other organ, except those involved in the excretory route (predominantly intestines). Finally, stomach values after 4 h were low (0.52 ± 0.34% ID per g) indicating minimal *in vivo* reoxidation to $^{99m}TcO_4^-$.

Conclusions

We have successfully directly incorporated a topoisomerase and tyrosine kinase inhibitor, an erlotinib analogue, in both Re and ^{99m}Tc complexes with minimal alteration of the analogue's molecular structure. We also report the biological studies of the resulting rhenium and ^{99m}Tc sandwich complexes, bearing an almost unmodified drug. Interestingly, only [Re(η^6-pseudoerlotinib)$_2$]$^+$ showed the ability to inhibit cell growth, while [Re(η^6-bz)(η^6-pseudoerlotinib)]$^+$ is almost inactive. In fact, the presence of two moieties of erlotinib seems to have a beneficial effect since the IC_{50} values of **1** are more than ten times smaller than **3**. This different behavior might reflect the better ability of **1** to enter the tumor cells and induce cell death. Finally, [^{99m}Tc(η^6-pseudoerlotinib)$_2$]$^+$ proved to be highly stable both *in vitro* and *in vivo*, being cleared through the hepatobiliary tract.

The synthetic concept proposed in this work is broadly applicable and serves as a general procedure towards other quinazoline-type EGFR and topoisomerase inhibitors such as Gefitinib and Vatalanib.

Experimental part

Materials and methods

Unless otherwise stated, all chemicals were of reagent grade or higher, obtained from commercial sources and used without further purification. Solvents for reactions were of p.a. grade or distilled prior to their use; H_2O was bi-distilled. Deuterated NMR-solvents were purchased from Armar Chemicals or Cambridge Isotope Laboratories, Inc. (UK). Reactions were carried out using standard Schlenk techniques in oven-dried (150 °C) glass equipment and monitored for completion by analyzing a small sample (after suitable workup) by UPLC-ESI-MS. Evaporation of the solvents *in vacuo* was done with the rotary evaporator. Microwave assisted reactions were carried out in a Biotage Initiator microwave. [Re(η^6-(aniline)$_2$)]PF_6 and **L1** were synthesized according to a literature procedure.[24,25]

^{1}H- and ^{13}C-NMR spectra. BrukerAV2-400 (400 MHz); in deuterated solvents at 300 K; chemical shifts (δ) in ppm relative to residual solvent resonances (acetone-d_6 ^{1}H: δ 2.05, ^{13}C: δ 29.84, CD_3OD ^{1}H: δ 3.31, ^{13}C: δ 49.00); coupling constants (J) in Hz.

HR-ESI-MS. QExactive (Thermo Fisher Scientific, Bremen, Germany) equipped with a heated ESI source connected to a Dionex Ultimate 3000 UPLC system. Samples dissolved in MeOH, MeOH/CH_2Cl_2 3 : 1, MeOH/H_2O 1 : 1, DMSO/H_2O 1 : 10, or H_2O at *ca.* 50 μg mL^{-1}; injection of 1 μLon-flow with an XRS auto-sampler (CTC, Zwingen, Switzerland)(mobile phase: MeOH + 0.1% HCOOH or CH_3CN/H_2O (2 : 8) + 0.1% HCOOH; flow rate 120 μL mL^{-1}); ion source parameters: sprayvoltage 3.0 kV, capillary temperature 280 °C, sheath gas 30 L min^{-1}, s-lens RF level 55.0; aux gas temperature 250 °C; full scan MS in alternating (+)/(−)-ESI mode; mass ranges 80–1200, 133–2000, or 200–3000 amu; resolution (full width half-maximum) 70 000; automatic gain control(AGC) target 3.00 × 10^6; maximum allowed ion transfer time(IT) 30 ms; mass calibration < 2 ppm accuracy for m/z 130.06619–1621.96509 in (+)-ESI with Pierce® ESI calibration solutions (Thermo Fisher Scientific, Rockford, USA); lock masses: ubiquitous erucamide (m/z 338.34174, (+)-ESI).

UPLC-ESI-MS. Waters Acquity UPLC System coupled to a Bruker Daltonics HCT™ESI-MS, using an Acquity UPLC BEH C18 1.7 μm (2.1 × 50 mm) column. UPLC solvents were formic acid (0.1% in millipore water) (solvent A) and acetonitrile UPLC grade (solvent B). Applied UPLC gradient: 0–0.5min: 95% A, 5% B; 0.5–4.0min: linear gradient from 95% A, 5% B to 0% A, 100% B; 4.0–5.0 min: 0% A, 100% B. The flow rate was 0.6 mL min^{-1}. Detection was performed at 250 and 480 nm (DAD).

Preparative HPLC. Shimadzu eco LC-20AP system, using a Dr Maisch Reprosil C18100-7 (40 × 250 mm) column for complex **2**. HPLC solvents were trifluoroacetic acid (0.1%in Millipore water) (solvent A) and HPLC grade acetonitrile (solvent B), with a flow rate 40 mL min^{-1}.

Gradient for [Re(η^6-bz)(η^6-aniline)]$^+$ (**2**) (**G2**): detection at 260 nm, 0–5 min: 75% A (25% B); 5–40 min: linear gradient from 75% A (25% B) to 60% A (40% B); 40–45 min: 60% A (40% B) to 0% A (100% B); 45–55 min: 100% B.

Radiochemistry. ***Caution!*** ^{99m}Tc is a radioactive isotope. All operations dealing with ^{99m}Tc must be carried out in a licensed and appropriately equipped laboratory, including state of the art radiation protection measures.

Na[$^{99m}TcO_4$] in 0.9% saline was eluted from a ^{99}Mo/^{99m}Tc Ultratechnekow® FM generator purchased from b.e. imaging AG (Switzerland).

HPLC analyses of ^{99m}Tc complexes. Merck Hitachi Chromaster 5160 pump coupled to a Merck Hitachi Chromaster 5430 diode array detector and a radiodetector. UV-vis detection was performed at 250 nm. The detection of radioactive ^{99m}Tc complexes was performed with a Berthold FlowStar LB 514 radiodetector equipped with a *BGO-X* cell. Separations were achieved on a Macherey-Nagel NUCLEOSIL®C18 5 μm, 100 Å (250 × 3 mm) column. HPLC solvents were trifluoroacetic acid (0.1% in Millipore water) (solvent A) and HPLC grade acetonitrile (solvent B). Applied HPLC gradient for purification of [^{99m}Tc(aniline)$_2$]$^+$, [^{99m}Tc(pseudoerlotinib)$_2$]$^+$ and the co-injection [^{99m}Tc(pseudoerlotinib)$_2$]$^+$ (**G1**): 0–3min: 95% A (5% B); 3–3.1 min: 95% A (5% B) to 75% A (25% B); 3.1–9 min: 75% A (25% B); 9–9.1 min: 75% A (25% B) to 66% A (34% B); 9.1–20 min: 66% A (34% B) to 0% A (100% B); 20–25 min: 0% A (100% B).

Syntheses

Synthesis of [Re(η^6-pseudoerlotinib)$_2$]PF_6 (1)PF_6. [Re(η^6-(aniline)$_2$)]PF_6 (10 mg, 0.018 mmol) was partially dissolved in 1 mL of HCl 0.2 M and mixed with **L1** (6.85 mg, 0.038 mmol, 1.1 eq.) in a round bottom flask, which was heated at 70 °C for 16 h. After 5 h crystals, suitable for X-ray diffraction analysis, started to form. They were filtered and washed with acetone. KOH was added to neutralize the solution and the aqueous phase was extracted with DCM (5 × 0.5 mL). The solvent was removed under vacuum; after the addition of NH_4PF_6 (5 mg, 0.03 mmol) to a water solution, **1PF$_6$** was extracted with DCM (4 × 0.5 mL), the solvent was removed under vacuum to obtain **1PF$_6$** (15 mg, 78%) as a pale-yellow solid. ^{1}H NMR (400 MHz, acetone-d_6): δ 8.46 (s, 2H, *H5*), 7.30 (d, J = 5.8 Hz, 4H, H_o), 6.97 (s, 2H, *H5*), 6.77 (s, 2H, *H10*), 6.19 (dd, J = 6.1, 5.0 Hz, 4H, H_m), 5.87 (t, J = 5.1 Hz, 2H, H_p), 4.42–4.29 (m, 4H, CH_2), 3.96 (dd, J = 5.6, 3.7 Hz, 4H, CH_2), 3.92–3.84 (m, 4H, CH_2), 3.48 (s, 6H, CH_3), 3.45 (s, 6H, CH_3).^{1}H NMR (500 MHz, CD_3OD) δ 8.64 (s, 2H, H2), 7.37 (m, 6H, H5 + Ho), 6.95 (s, 2H, H10), 6.25 (t, J = 5.5 Hz, 4H, Hm), 5.90 (t, J = 5.3 Hz, 2H, Hp), 4.36 (d, J = 5.0 Hz, 4H, CH_2), 4.12 (d, J = 5.1 Hz, 4H, CH_2), 3.91–3.84 (m, 8H, CH_2), 3.51 (s, 6H, CH_3), 3.49 (s, 6H, CH_3). ^{13}C NMR from the HSQC spectrum (CD_3OD): δ 149.9 (*C2*), 103.5 (*C10*), 103.2 (*C5*), 76.3 (C_o), 76.1 (C_m), 75.8 (C_p), 71.6 (*C*H$_2$), 71.5 (*C*H$_2$), 70.6 (*C*H$_2$), 70.2 (*C*H$_2$), 59.3 (*C*H$_3$), 59.2 (*C*H$_3$). HRMS (ESI$^+$) m/z calcd For $C_{40}H_{46}N_6O_8Re^+$ [M]$^+$: 925.29291, found: 925.29042.

Synthesis of [Re(η^6-aniline)(η^6-benzene)]PF_6 (2)PF_6. [Re(bz)(napht)]PF_6 (30 mg, 0.056 mmol) was partially dissolved in 2 mL of dioxane and mixed with aniline (1 mL, 11.15 mmol, in excess) and NMP (13.44 μL, 0.139 mmol, in excess) in a Schlenk flask, which was heated at 120 °C for 1.5 h. The solvent was removed *under vacuum* and the residue was washed with Et_2O (3 × 2 mL) purified by preparative RP-HPLC gradient (**G2**) and freeze-dried to afford **2TFA** (16 mg, 57%) as a pale-yellow solid. Single crystals, suitable for X-ray diffraction analysis were obtained by vapour diffusion from Et_2O (antisolvent) into methanol (solvent). ^{1}H NMR (400 MHz, CD_3OD): δ 6.06 (m, 2H$_o$), 5.97 (m, 2H$_m$), 5.71 (t, J = 5.2 Hz, 1H$_p$), 5.67 (s, 6H, benzene). ^{1}H NMR (400 MHz, acetone-d_6): δ 6.25 (d, J = 5.9 Hz, 2H*o*), 6.08 (dd, J = 6.1, 5.0 Hz, 2H$_m$), 5.82 (t, J = 5.2 Hz, 1H$_p$), 5.76 (s, 6H, benzene), 5.10 (br s, 2H, NH_2). ^{13}C NMR from the HSQC spectrum (acetone-d_6): δ 77.3 (C$_p$), 75.9 (C$_m$), 75.1 (benzene), 65.2 (C$_o$). HRMS (ESI$^+$) m/z calcd For $C_{12}H_{13}NRe$ [M]$^+$: 358.06000, found: 358.06006.

Synthesis of [Re(η^6-pseudoerlotinib)(η^6-benzene)]PF_6 (3)PF_6. (2)PF_6 (10 mg, 0.020 mmol) was partially dissolved in 1 mL of HCl 0.2M and mixed with **L1** (6.85 mg, 0.022 mmol, 1.1 eq.) in

a round bottom flask, which was heated at 70 °C for 16 h. KOH was added to neutralize the solution and the aqueous phase was extracted with DCM (5 × 0.5 mL). The solvent was removed under vacuum; after the addition of NH_4PF_6 (5 mg, 0.03 mmol) to a water solution, **3PF$_6$** was extracted with DCM (4 × 0.5 mL), the solvent was removed under vacuum to obtain xxPF_6 (10 mg, 75%) as a pale-yellow solid. Single crystals, suitable for X-ray diffraction analysis were obtained by vapour diffusion from Et_2O (antisolvent) into DCM (solvent). ^{1}H NMR (400 MHz, acetone-d_6): δ 8.68 (s, 1H, *H2*), 7.55 (s, 1H, *H5*), 7.32 (s, 1H, H10), 7.19 (d, J = 5.8 Hz, 2H, H_o), 6.32 (t, J = 5.6 Hz, 2H, H_p), 6.05 (m, 7H, H_p + C*H* benzene), 4.40–4.31 (m, 2H, CH_2), 4.26–4.18 (m, 2H, CH_2), 3.88–3.75 (m, 4H, CH_2), 3.42 (s, 3H, CH_3), 3.41 (s, 3H, CH_3). ^{13}C NMR from the HSQC spectrum (acetone-d_6): δ 152.7 (*C2*), 108.6 (*C10*), 103.1 (*C5*), 77.4 (*C*H benzene + C_p), 75.6 (C_m), 72.8 (C_o), 71.2 (*C*H$_2$), 69.6 (*C*H$_2$), 69.3 (*C*H$_2$), 58.8 (*C*H$_3$). HRMS (ESI$^+$) *m*/*z* calcd For $C_{26}H_{29}N_3O_4Re^+$ [M]$^+$: 634.17101, found: 634.17143.

Pseudoerlotinib (L2). L1 (100 mg, 0.320 mmol) was dissolved in 2 mL of HCl 0.2 M and mixed with aniline (44.7 μL, 0.481 mmol) and heated at 70 °C. After a few minutes an abundant precipitate formed that was filtered and washed with cold water. The precipitate was then partially dissolved in water and neutralized with a saturated solution of $NaHCO_3$. The water solution was extracted with DCM (3 × 10 mL), dried over $MgSO_4$ anhydrous and the solvent was removed under reduced pressure, yielding 106 mg (90%) of white powder. ^{1}H NMR spectrum was in agreement with the literature data.[25]

Synthesis of [^{99m}Tc(η^6-aniline)$_2$]$^+$. Method A:[22] Zn (20 mg turnings), SDS (4 mg), aniline (20 μL, 0.2 mmol), 3N HCl (50 μL), were added into the vial. The vial was sealed and flushed with N_2 for 1 min. Na[^{99m}TcO$_4$] (1 mL) was added, the vial was flushed with N_2 for 1 min, and heated at 100 °C (μwave) for 30 min. The separation of the ^{99m}Tc products from excess ligand or residual [^{99m}TcO$_4$]$^-$ was achieved by analytical HPLC. To obtain a pure compound, the ^{99m}Tc product was collected.

Method B: Zn (20 mg turnings), SDS (4 mg), aniline (20 μL, 0.2 mmol), 3N HCl (50 μL), were added into the vial. The vial was sealed and flushed with N_2 for 1 min. Na[^{99m}TcO$_4$] (1 mL) was added, the vial was wasflushed with N_2 for 1 min, and heated at 80–85 °C (sonicator) for 1 h. The solution was neutralized by addition of NaOH 1 M (~10 drops) and washed with Et_2O (1 mL × 8).

Synthesis of [^{99m}Tc(η^6-pseudoerlotinib)$_2$]$^+$ ([^{99m}Tc]1). To a [^{99}mTc(η^6-aniline)$_2$]$^+$ solution was added **L1** (4 mg, 0.013 mmol) and 3N HCl (20 μL). The vial was sealed and flushed with N_2 for 1 min and heated at 120 °C for 30 min. To get clean co-injections, the ^{99m}Tc products were collected from the HPLC and then mixed with the Re homologues.

***In vitro* stability studies.** Radiochemical stability of [^{99m}Tc]**1** was assessed by RP-HPLC analysis following 24 h incubation of the compound in PBS pH 7.4 and in DMEM cell culture medium at 37 °C, respectively.

Log *D* measurement. Octanol/water partition coefficient were evaluated such that analytes were added in aqueous solution to an equal volume of *n*-octanol. After vigorous mixing, the phases were separated, and the radioactivity of each phase was evaluated. Under the assumption that the radioactivity determined in each phase correlated directly with the concentration within it, eqn (1) was used to evaluate K_{OW} where $[O]_{eq}$ was the radioactivity recorded in the *n*-octanol phase at equilibrium and $[W]_{eq}$ the respective water radioactivity. The remaining activity of empty containers was subtracted from the total activity. Each K_{OW} value was indicated as an average of three sets of measurements, recorded on the same day and from the same labeling experiment.

$$K_{OW} = \frac{[O]_{eq}}{[W]_{eq}} \quad (1)$$

Cellular studies

Cell culture. The human epidermoid carcinoma A431 cells (ATCC® CRL-1555™) were grown in Dulbecco's modified Eagle's medium (DMEM) containing GlutaMax I supplemented with 10% heat-inactivated fetal bovine serum (FBS) and 1% penicillin/streptomycin antibiotic solution (Gibco, Thermo Fisher Scientific, Waltham, MA, USA). Cells were cultured in a humidified atmosphere of 95% air and 5% CO_2 at 37 °C (Heraeus, Germany) and tested for mycoplasma using the LookOut® mycoplasma PCR Detection kit.

Cytotoxicity evaluation. The cytotoxicity of the Re complexes **1** and **3**, and the ligand **L2** was assessed by evaluating their effects on cellular proliferation using the [1-(4,5-dimethylthiazol-2-yl)-2,5-diphenyl tetrazolium] (MTT) assay. A431 cells were seeded in 96-well culture plates at a density of 2.5 × 10^4 cells per well and left to adhere overnight at 37 °C. Cells were then incubated with the tested compounds at different concentrations (0.01, 0.05, 0.1, 0.5, 1, 5, 10, 20, 50, 100 μM) during 48 h at 37 °C. All tested compounds were first solubilized in DMSO (20 mM stock solution) and then diluted in culture medium for the assay, with the percentage of organic solvent in the final solution never exceeding 0.1%. After incubation, the medium was removed, the cells were washed with PBS and then incubated with MTT (200 μL of 0.5 mg mL^{-1} solution in MEM without phenol red) for 3 h at 37 °C. The MTT solution was then removed and the insoluble blue formazan crystals formed were dissolved in DMSO. The absorbance of this colored solution was measured at 570 nm in a plate spectrophotometer (Power Wave Xs; Bio-Tek). Each test was performed with at least six replicates. The results were expressed as the percentage of the surviving cells in relation to the control, which was incubated without any compound. IC_{50} values were determined using Graph Pad Prism.

Cellular uptake by ICP-MS. Cellular uptake of the Re complexes was assessed by ICP-MS quantification of total rhenium. A431 cells were plated at a density of one million cells per well of a 6-well plate in culture medium and allowed to attach overnight. Then, the medium was removed and cells were incubated with the tested compounds (50 μM) for 24 h. The harvested cell suspension was centrifuged at 200*g* for

3 min at 4° C (Centrifuge 5804R, Eppendorf) and cells were washed twice with cold PBS to remove the unbound complexes. An aliquot of 10 μL of cells suspension was separated for counting the number of cells with trypan blue. The Re content of the pellet was determined by ICP-MS, as a service provided by Laboratório Central de Análises/Universidade de Aveiro. The concentration of Re was calculated as ng of metal per million of cells. Each complex was tested in triplicate and data are presented as average ± SEM.

Biodistribution studies. Animal studies were conducted in conformity with national law and with the EU Guidelines for Animal Care and Ethics in Animal Experimentation. The animals were housed in a temperature- and humidity-controlled room with a 12 h light/12 h dark schedule. Biodistribution of the ^{99m}Tc complexes was estimated by intravenous (tail vein) injection of the compound diluted (1–4 MBq) in 100 μL of PBS pH 7.2 in healthy CD1 female mice. The animals (n = 3 per time point) were killed by cervical dislocation at 1 and 4 h after injection. The dose administered (injected activity) as well as the radioactivity in the sacrificed animals were measured using a dose calibrator (Carpintec CRC-55TW, Ramsey, USA). The total excretion corresponds to the difference between those radioactivities. Normal organs (brain, heart, spleen, lungs, liver, kidneys, intestine, stomach, and pieces of muscle and bone) were dissected, rinsed with saline to remove excess blood, weighed, and counted on a γ-counter (LB2111, Berthold, Germany). The organ uptake was calculated as the percentage of the injected dose per gram of organ mass (%ID per g) or the percentage of injected dose per organ (%ID per organ). For blood, bone, and muscle, total activity was estimated assuming that these organs constitute 6, 10 and 40% of the total body weight, respectively.

Author contributions

F. B. conceptualized the project, performed the experiments, data acquisition and analysis, wrote and edited the manuscript; C. F. and P. D. R. performed the biological experiments; O. B. performed all crystallographic measurements; A. P. conceptualized the biological experiments; R. A. conceptualized the project and edited the manuscript. Additional edits and proof reading were conducted by all authors. All authors have read and agreed to the published version of the manuscript.

Abbreviations

Bz	Benzene
DCM	Dichloromethane
DMEM	Dulbecco's modified Eagle's medium
DMSO	Dimethyl sulfoxide
FBS	Fetal bovine serum
GFR	Epidermal growth factor receptor
ESI	Electrospray ionization
Et_2O	Diethyl ether
IC_{50}	Half maximal inhibitory concentration
ICP-MS	Inductively coupled plasma mass spectrometry
HPLC	High-performance liquid chromatography
HR	High-resolution
MS	Mass spectrometry
napht	Naphthalene
MTT	[1-(4,5-Dimethylthiazol-2-yl)-2,5-diphenyl tetrazolium]
NMP	*N*-Methyl-2-pyrrolidone
NMR	Nuclear magnetic resonance
PBS	Phosphate-buffered saline
SDS	Sodium dodecyl sulfate
TFA	Trifluoroacetic acid
TKI	Tyrosine kinase inhibitor.

Conflicts of interest

There are no conflicts to declare.

Acknowledgements

We thank the University of Zurich for financial support.

References

1 J. L. Nitiss, *Nat. Rev. Cancer*, 2009, **9**, 327–337.
2 J. C. Wang, *Nat. Rev. Mol. Cell Biol.*, 2002, **3**, 430–440.
3 J. L. Nitiss, *Nat. Rev. Cancer*, 2009, **9**, 338–350.
4 J. V. Walker and J. L. Nitiss, *Cancer Invest.*, 2002, **20**, 570–589.
5 D. S. Krause and R. A. Van Etten, *Eur. J. Cancer*, 2005, **38**, 172–187.
6 R. I. Nicholson, J. M. W. Gee and M. E. Harper, *Eur. J. Cancer*, 2001, **37**, 9.
7 S. V. Sharma, D. W. Bell, J. Settleman and D. A. Haber, *Nat. Rev. Cancer*, 2007, **7**, 169–181.
8 M. Chauhan, G. Sharma, G. Joshi and R. Kumar, *Curr. Pharm. Des.*, 2016, **22**, 3226–3236.
9 Ž. Skok, N. Zidar, D. Kikelj and J. Ilaš, *J. Med. Chem.*, 2020, **63**, 884–904.
10 W. Cai, G. Niu and X. Chen, *Eur. J. Nucl. Med. Mol. Imaging*, 2008, **35**, 186–208.
11 C. Arteaga, *Semin. Oncol.*, 2003, **30**, 3–14.
12 R. D. Mass, *Int. J. Radiat. Oncol., Biol., Phys.*, 2004, **58**, 932–940.
13 J. Albanell and P. Gascón, *Curr. Drug Targets*, 2005, **6**, 259–274.
14 D. Vallböhmer and H. J. Lenz, *Clin. Colorectal Cancer*, 2005, **5**, S19–S27.
15 D. N. Tran, A. Zhdanko, S. Barroso, P. Nieste, R. Rahmani, J. Holan, R. Hoefnagels, P. Reniers, F. Vermoortele, S. Duguid, L. Cazanave, M. Figlus, C. Muir, A. Elliott, P. Zhao, W. Paden, C. H. Diaz, S. J. Bell, A. Hashimoto,

A. Phadke, J. A. Wiles, I. Vogels and V. Farina, *Org. Process Res. Dev.*, 2022, **26**, 832–848.
16 E. B. Corcoran and R. N. Hanson, *Med. Res. Rev.*, 2014, **34**, 596–643.
17 A. Bourkoula, M. Paravatou-Petsotas, A. Papadopoulos, I. Santos, H. J. Pietzsch, E. Livaniou, M. Pelecanou, M. Papadopoulos and I. Pirmettis, *Eur. J. Med. Chem.*, 2009, **44**, 4021–4027.
18 C. Fernandes, I. C. Santos, I. Santos, H. J. Pietzsch, J. U. Kunstler, W. Kraus, A. Rey, N. Margaritis, A. Bourkoula, A. Chiotellis, M. Paravatou-Petsotas and I. Pirmettis, *Dalton Trans.*, 2008, 3215–3225.
19 C. Kiritsis, A. Shegani, K. Makrypidi, I. Roupa, A. Lazopoulos, A. Panagiotopoulou, S. Triantopoulou, M. Paravatou-Petsotas, H. J. Pietzsch, M. Pelecanou, M. Papadopoulos and I. Pirmettis, *Bioorg. Med. Chem.*, 2022, **73**, 117012.
20 K. Makrypidi, C. Kiritsis, I. Roupa, S. Triantopoulou, A. Shegani, M. Paravatou-Petsotas, A. Chiotellis, M. Pelecanou, M. Papadopoulos and I. Pirmettis, *Molecules*, 2023, **28**, 1–15.
21 E. P. Kündig, C. Perret, S. Spichiger and G. Bernardinelli, *J. Organomet. Chem.*, 1985, **286**, 183–200.
22 Q. Nadeem, G. Meola, H. Braband, R. Bolliger, O. Blacque, D. Hernández-Valdés and R. Alberto, *Angew. Chem., Int. Ed.*, 2020, **59**, 1197–1200.
23 Q. Nadeem, F. Battistin, O. Blacque and R. Alberto, *Chem. – Eur. J.*, 2022, **28**, 1213–1216.
24 J. Csucker, D. K. Jo, Q. Nadeem, O. Blacque, T. Fox, H. Braband and R. Alberto, *Dalton Trans.*, 2022, **51**, 9591–9595.
25 L. Barghi, A. Aghanejad, H. Valizadeh, J. Barar and D. Asgari, *Adv. Pharm. Bull.*, 2012, **2**, 119–122.
26 F. Azmian Moghadam, M. Evazalipour, H. Kefayati and S. Ghasemi, *Pharm. Sci.*, 2021, **27**, 209–218.